Indian Journal of Chemistry
Vol. 59B, March 2020, pp. 385-392

Experimental study of end-capped acceptors influencing the photo-physical, electrochemical and thermal parameters of A-D-π-D-A type small molecular electron donors

Ejjurothu Appalanaidu, Manohar Reddy Busireddy, B V Subba Reddy & Vaidya Jayathirtha Rao*

Fluoro and Agrochemicals Division and AcSIR, CSIR-Indian Institute of Chemical Technology, Hyderabad 500 007, India

E-mail: vaidya.opv@gmail.com; basi reddy@csiriict.res.in

Received 24 August 2019; accepted (revised) 13 January 2020

We have designed A-D-π-D-A type three new small molecular donor materials denoted as **FD-IND**, **FD-DCV** and **FD-NBR**, which have been synthesised and their photo-physical, electrochemical and thermal properties explored. The synthesised materials have fluorene as "π-spacer," dithieonopyrrole as "Donor" (D) and various "Acceptor" (A) units are 1,3-indanedione (IND), dicyanovinylene (DCV) and N-butyl rhodanine (NBR). All these three materials have good solubility (~30 mg/mL) in most common organic solvents and have relatively broad absorption in the visible region covering the range of 300-650 nm with two primary absorption bands. The absorption bands located at shorter wavelength region are ascribed to a localized aromatic π-π* transition of the A-D-π-D-A system, while the bands at longer wavelength are mainly attributed to an ICT transition. All the compounds exhibit excellent thermal stabilities in the range of 260-373°C. Cyclic voltammetry data provided HOMO values as −5.26, −5.32 and −5.32 eV for **FD-NBR**, **FD-DCV** and **FD-IND** respectively. LUMO values estimated from HOMO values and optical band gap are −3.27, −3.22 and −3.37 eV for **FD-NBR**, **FD-DCV** and **FD-IND** respectively. Therefore, these are potential molecules for organic solar cells.

Keywords: Dithienopyrrole-fluorene, A-D-π-D-A type structure, end-capped acceptors, organic solar cell material

Bulk hetero junction solar cells (BHJSCs) are considerable promising entrant in future energy source due to cost effective, lightweight, solution processable fabrication, environmentally friendly energy-converting devices and easily coated on flexible substrate[1-5]. Small molecular electron donors (SMEDs) based on D- π -A- π -D[6a], D-(π)A-A[7,8], D-A-D[9,10], star and funnel-shaped[11,12] A-D-D'-D-A[13-15] frameworks have been reported in the realm of organic photovoltaics (OPV), A- π -D- π -A type molecular systems are proven as the valid designed framework to exhibit the excellent power conversion efficiency (PCE)[16-18]. Over the past decades, multitudinous efforts have been devoted to synthesize various SMEDs based on this framework[19]. Recently, extension of this model into the development of non-fullerene small molecular electron acceptors (NFSMEAs)[20,21] become a successful strategy to outperform the expensive phenyl-C_{61}-butyric acid methyl ester ($PC_{61}BM$) or phenyl-C_{71}-butyric acid methyl ester ($PC_{71}BM$) electron acceptors[20,22-24]. Gratifyingly, as an active layer, combination of SMED-SMEA systems based on A- π -D- π -A framework reached the PCE plateau of ~15%[17,22,25]. This could be mainly attributed to the electron acceptors and attaching them at the terminal position leading to (i) greater intra-molecular charge transfer (ICT) on both directions of the peripheral sides during photo-excitation; (ii) effective exciton transport and its dissociation at D-A interface and (iii) act as π-stacking regulators to govern the intermolecular interactions[2]. Astonishingly, blending of A- π -D- π -A type NFSMAs with polymers yielded the impressive photo-conversion efficiency (PCE) of 16% for a single junction device[26] and 17.3% for the tandem device respectively in the recent years[27]. It can be said that the day is not far off to commercialize these promising candidates for future energy needs. Also, we believe in that still there is a possibility to increase the PCE through modulation on terminal acceptor units or introducing new acceptor units into this framework.

To design novel acceptor systems, prerequisite is to get a detailed understanding about their structure-property relationship at the molecular level. Till to date, a vast number of A- π -D- π -A type SMEDs containing various terminal acceptor units including N-alkyl rhodanine (NAR)[13,14,16,25,28], dicyanovinylene

(DCV)[29,30], cyanoethylacetate (CA)[31], 1,3-indanedione (IND)[15,32], thiobarbituric acid (BA)[33], thieno[2,3-c]pyrrole-4,6-dione (TPD)[34] and 2-(1,1-dicyanomethylene)rhodanine (RCN)[35] have been studied for BHJSCs applications. Based on a series of research exploration, we have found that the PCE produced by NAR and IND units is significantly high over the any other of its counterparts[29,31,32,36-38]. For instance, Deng *et al*. developed a series of A- π -D- π -A type molecules containing four various end-capped acceptor units. Of these, compounds containing NAR and IND units yielded the highest PCE of 9.6% and 10.1% respectively as compared to the RCN and BA acceptors[33]. Antwi *et al*. demonstrated the greater PCE of IND and NBR end-capped molecules over the CA counterpart[32]. Jangkeun and co-workers also found nearly similar pattern of PCE with respect to terminal acceptor units *i.e*., IND > NAR > DCV > CA[29]. Guankui *et al*. reported a series of quinquethiophene derivatives with various acceptors and NAR end-capped A- π -D- π -A system secured the highest position in terms of PCE[36]. Closer scrutinization on their I-V measurements witnessed the remarkable photovoltaic performance of IND and NAR units mainly originates from their larger short-circuit current (J_{SC}). In addition, comparatively high PCE of IND unit in the series is assigned to its large dipole moment variation from ground to excited state because it weakens the Coulombic attraction between the hole and electron thereby facilitates charge separation at the D-A interface[39]. This variation reflects in V_{OC} which in turn affecting the photovoltaic performance to a certain extent[33].

To delve the effect of end-capped acceptor units on structural, charge transfer/transport and spectroscopical features, we have adopted a novel A- D - π - D -A framework by interchanging donor and π-linker's position of the mostly studied A- π -D- π -A system. Using this framework, we have synthesized and characterized three molecules comprised of a common donor and spacer unit but varied the terminal acceptor units namely N-butyl rhodanine (NBR), dicyanovinylene (DCV) and 1,3-indanedione (IND) (Figure 1). In this study, fluorene was chosen as a spacer unit at the central position because of its unique aromatic nature to increase the light harvesting ability along with HOMO stabilization which is proportional to V_{OC} and oxidative stability[6a,8]. The dioctyl group substitution at 9, 9'-positions of fluorene not only used to enhance the solution processability, to avoid the intermolecular π-π aggregation and film texture, hence minimizing the charge recombination. Selection of appropriate chemical functionalities for the proper alignment of D-A units in the conjugated skeleton is of crucial importance to achieve the desired characteristic features such as photo-physical properties, frontier energy levels, charge transport and morphology. Hence, planar dithieno[3,2-b:2', 3'-d]pyrrole (DTP) as donor unit was chosen and flanking them with fluorene in the framework shifted of absorption wavelength to visible region, because, greater heteroatomic functionalities on DTP possessing non-bonding electrons that can increase the number of low energy n-π* transitions, thereby improving the light harvesting ability[9]. In addition, DTP is reported to have excellent hole transport and thermal stability than its congener carbazole[6a,8]. Branched N-ethylhexylation of DTP offers better solubility and reduces the aggregation. Conventional Suzuki coupling approach was used to connect the fluorene and DTP segments using $Pd(PPh_3)_4$ as catalyst. Target compounds have been synthesized *via* Knoevenagel condensation. Synthesized materials were characterized using various analytical techniques to examine the energy levels, photo-physical, electrochemical and thermal properties.

Experimental Section

All the reactions were carried out under nitrogen atmosphere. All the reagents were of reagent/analytical grade and used without further purification. Solvents used in this work such as freshly distilled tetrahydrofuran (THF) (distilled over sodium and benzophenone), dry Toluene (dried on sodium wire) and N,N-dimethylformamide (DMF) was dried over 3 Å molecular sieves to remove the moisture under

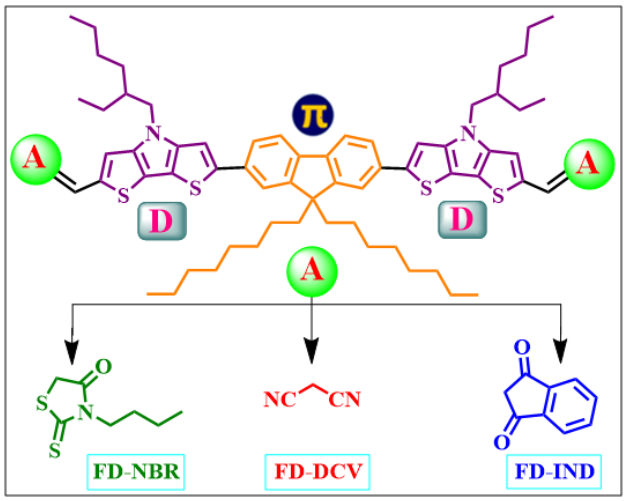

Figure 1 — Schematic molecular representation of the compounds based on A-D-π-D-A configuration

nitrogen atmosphere. All chromatographic separations were carried out on silica gel (100-200 mesh). ^{1}H and ^{13}C NMR spectra were recorded on a Bruker Avance DPX spectrometer using $CDCl_3$ solvent with TMS as internal standard. MALDI-TOF/TOF spectrometer (Shimadzu) was used to obtain the mass spectral data for the target compounds. UV-vis absorption spectra were recorded using a Cary 5000 UV-VIS-NIR spectrophotometer and Cary Eclipse fluorescence spectrophotometer has been used for the fluorescence experiments. Cyclic voltammetry measurements were performed on a PC-controlled CHI 62C electrochemical analyzer using 1 mM dye solution in CH_2Cl_2 at a scan rate of 1000 mVs^{-1} using 0.1 M tetrabutylammonium perchlorate (TBAP) as supporting electrolyte. The glassy carbon, standard calomel electrode (SCE) and platinum wire were used as working, reference and auxiliary electrodes respectively. The potential of the reference electrode was calibrated using ferrocene internal standard. Thermogravimetric analyses (TGA) were performed with a TGA 7200 thermal analyzer with a heating rate of 10°C min^{-1}.DSC experiments were conducted using Exstar DSC 7020 instrument with a heating and cooling rate of 10°C min^{-1}.

Synthetic procedures

6,6'-(9,9-Dioctyl-9*H*-fluorene-2,7-diyl)bis(4-(2-ethylhexyl)-4*H*-dithieno[3,2-b:2',3'-d]pyrrole -2-carbaldehyde) (FDA)

6-Bromo-4-(2-ethylhexyl)-4*H*-dithieno[3,2-b:2',3'-d]pyrrole-2-carbaldehyde (**7**) (1.85 g, 2.88 mmoland 2,2'-(9,9-dioctyl-9*H*-fluorene-2,7-diyl)bis(4,4,5,5-tetramethyl-1,3,2-dioxaborolane) (**3**) (1 g, 2.5 mmol) dissolved in dry toluene (15 mL) were degassed under nitrogen atmosphere for 15 minutes followed by the addition of $Pd(PPh_3)_4$ (90 mg, 5 mol%) catalyst. The reaction solution was heated to 100°C with continuous stirring for 24 h. The obtained reaction mixture was filtered through the celite pad to remove the inorganic impurities and extracted with CH_2Cl_2. The organic layer was thoroughly washed with water and then dried over anhydrous Na_2SO_4. After the evaporation of solvent, the crude product was purified by column chromatography on a silica gel using a mixture of CH_2Cl_2 and petroleum ether (2:1) as eluent to afford the desired product as a yellow solid (1.20 g, 75%). ^{1}H NMR (500 MHz, $CDCl_3$): δ 0.71-0.80 (m, 12H), 0.89-0.92 (m, 6H), 0.94-0.98 (m, 6H), 1.09-1.19 (m, 18H), 1.30-1.43 (m, 16H), 2.03-2.09 (m, 6H), 4.12-4.16 (m, 4H), 7.27 (S, 2H), 7.60 (d, *J* = 1.2 Hz,2H), 7.62 (S, 2H), 7.66 (dd, *J* = 1.5 Hz, *J* = 1.5 Hz, 2H), 7.73 (d, *J* = 7.9 Hz, 2H), 9.88 (S, 2H); ^{13}C NMR (125 MHz, $CDCl_3$): δ 10.7, 13.9, 14.0, 22.5, 22.9, 23.7, 24.0, 28.5, 29.6, 30.5, 31.4, 40.3, 51.4, 55.3, 106.4, 114.0, 119.1, 119.8, 120.3, 123.5, 124.5, 133.8, 140.0, 140.7, 144.3, 147.9, 149.9,151.9, 182.7; MALDI-MS ('+' mode, *m/z*): Found: 1025.91 ($M+H^+$). Calcd: 1024.51.

(5Z,5'E)-5,5'-(((9,9-Dioctyl-9*H*-fluorene-2,7-diyl)bis(4-(2-ethylhexyl)-4*H*-dithieno[3,2-b:2',3'-d]pyrrole-6,2-diyl))bis(methaneylylidene))bis(3-butyl-2-thioxothiazolidin-4-one) (FD-NBR)

To the solution of dialdehyde compound (**FDA**) (0.8 g, 0.78 mmol) in chloroform (40 mL), N-butyl rhodanine (0.73 g, 4 mmol) and a catalytic amount of piperidine was added under an inert atmosphere. The resulting solution was heated to 40°C overnight and cooled to RT. The obtained reaction mixture was partitioned using water and chloroform. The organic layer was collected and aqueous layer was extracted with chloroform (4 × 35 mL). The combined organic extract was washed with brine and dried over anhydrous Na_2SO_4, filtered and concentrated under reduced pressure. The crude obtained was purified by silica gel column chromatography (40% chloroform in hexane as an eluent) to yield the title compound as pink solid (0.85 g, 80%). ^{1}H NMR (500 MHz, $CDCl_3$): δ 0.7-0.80 (m, 6H), 0.90-0.92 (m, 6H), 0.94-0.98 (m, 12H), 1.09-1.11 (m, 16H), 1.28-1.42 (m, 24H), 1.61-1.72 (m, 6H), 1.99-1.24 (m, 8H), 4.01-4.20 (m, 8H), 7.24 (S, 4H), 7.60 (S, 2H), 7.65 (d, *J* = 5.0 Hz, 2H), 7.71 (d, *J* = 6.5 Hz, 2H), 7.90 (S, 2H); ^{13}C NMR (125 MHz, $CDCl_3$): δ 10.7, 13.6, 13.9, 14.0, 20.0, 22.5, 22.9, 23.8, 24.0, 28.5, 29.0, 29.6, 30.5, 31.4, 40.3, 44.1, 44.5, 51.4, 55.3 106.3, 114.3, 116.5, 117.1, 119.6, 120.3, 123.0, 124.7, 127.0, 133.8, 135.1, 140.6, 145.4, 147.2, 148.8, 151.9, 167.4, 192.0; MALDI-TOF ('+' mode, *m/z*): 1367.58 ($M+H^+$). Calcd: 1366.55.

2,2'-(((9,9-Dioctyl-9*H*-fluorene-2,7-diyl)bis(4-(2-ethylhexyl)-4*H*-dithieno[3,2-b:2',3'-d] pyrrole-6,2-diyl))bis(methaneylylidene))dimalononitrile (FD-DCV)

This compound was synthesized according to the synthetic procedure of **FD-NBR** except that dicyanovinylene (0.32 g, 5 mmol) was used in lieu of N-butyl rhodanine to obtain the title compound as pink solid (1.04 g, 83%). ^{1}H NMR (500 MHz, $CDCl_3$): δ 0.72-0.78 (m, 12H), 0.89-0.92 (m, 6H), 0.94-0.98 (m, 6H), 1.06-1.14 (m, 14H), 1.28-1.41(m, 20H), 1.97-2.02 (m, 2H), 2.07-2.11 (m, 4H), 4.11-4.16 (m, 4H), 7.26 (S, 2H), 7.61 (S, 2H), 7.63

(S, 2H), 7.68 (dd, *J* = 1.2 Hz, *J* = 1.6 Hz, 2H). 7.72 (S, 2H), 7.76 (d, *J* = 7.93 Hz, 2H); ^{13}C NMR (125 MHz, $CDCl_3$): δ 10.7, 13.9, 14.0, 13.9, 22.5, 22.9, 23.7, 24.0, 28.5, 29.5, 29.6, 30.5, 31.4, 40.2, 40.4, 51.5, 55.0, 71.5, 106.4, 114.3. 114.7, 115.3, 120.0, 120.5, 125.1, 126.6, 132.2, 133.6, 141.1, 145.2, 150.5, 150.7, 151.8, 152.1; MALDI-TOF ('+' mode, *m/z*): (M+Na). Found: 1143.59. Calcd: 1120.53.

2,2'-(((9,9-Dioctyl-9*H*-fluorene-2,7-diyl)bis(4-(2-ethylhexyl)-4*H*-dithieno[3,2-b:2',3'-d] pyrrole-6,2-diyl))bis(methaneylylidene))bis(1*H*-indene-1,3(2*H*)-dione) (FD-IND)

This compound was synthesized according to the synthetic procedure of **FD-NBR** except that 1,3-indanedione (0.72 g, 5 mmol) was used in lieu of N-butyl rhodanine to obtain the desired product as pink solid (1.04 g, 83%). ^{1}H NMR (400 MHz, $CDCl_3$): δ 0.76-0.81 (m, 12H), 0.90-0.94 (m, 6H), 0.96-1.00 (m, 6H), 1.10-1.13 (m, 18H), 1.35-1.43 (m, 16H), 2.04-2.13 (m, 6H), 4.14-4.18 (m, 4H), 7.24 (S, 2H), 7.62 (S, 2H), 7.68-7.74 (m, 8H),7.89-7.96 (m, 8H); ^{13}C NMR (125 MHz, $CDCl_3$): δ 10.5, 13.7, 13.8, 22.3, 22.7, 23.5, 23.8, 28.3, 28.9, 29.4, 29.7, 30.3, 31.4, 40.0, 40.1, 51.1, 55.2, 106.1, 114.3, 119.6, 120.1, 122.1, 122.2, 124.7, 133.5, 133.9, 134.2, 135.4, 137.2, 139.7, 140.7, 141.7,149.6, 151.2, 151.8, 189.8, 190.5; MALDI-TOF ('+' mode, *m/z*): 1281.56 ($M+H^+$). Calcd: 1280.56.

Results and Discussion

Synthesis

All the target compounds were prepared according to a multiple synthetic pathway as depicted in Scheme I. Synthesis was initiated with the

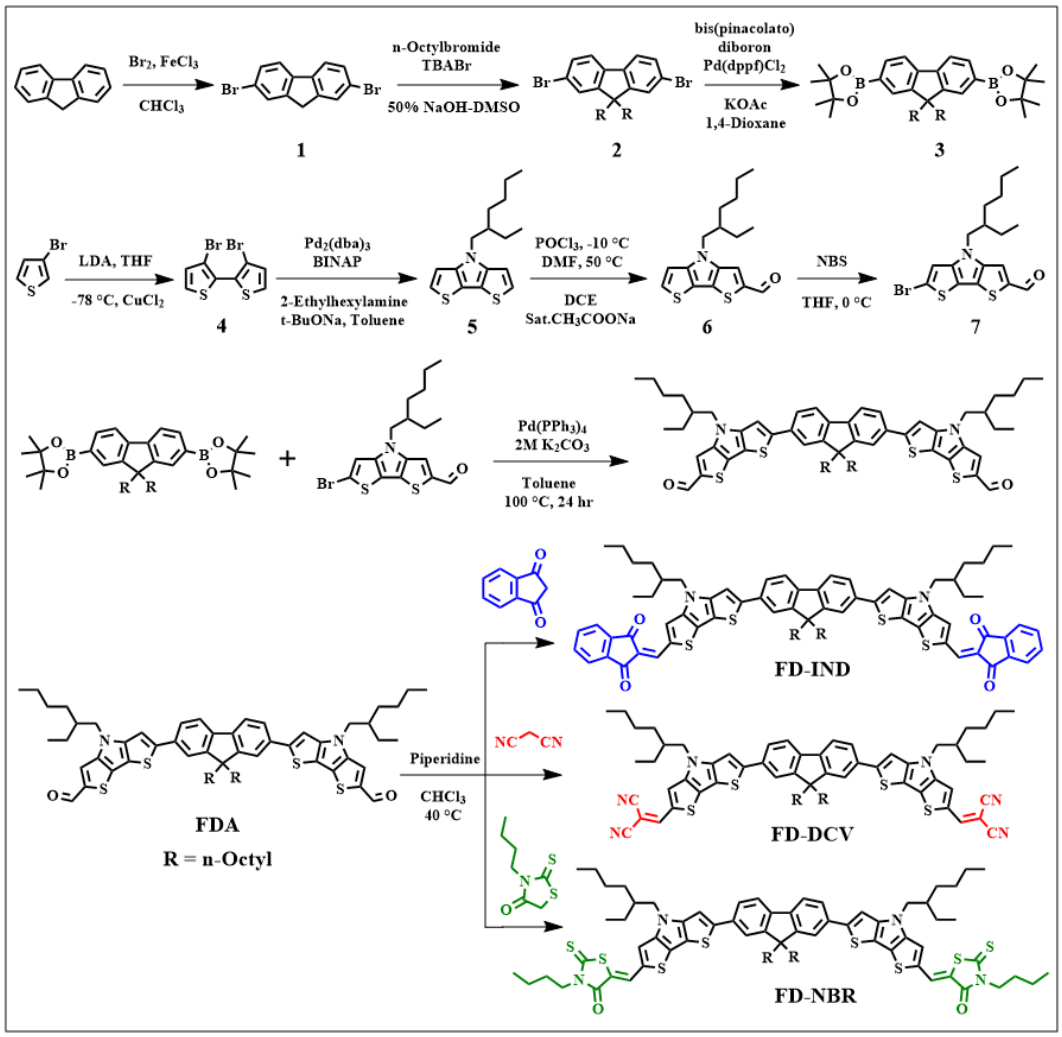

Scheme I — Synthetic pathway for the preparation of the target compounds

bromination of commercially available fluorine (**1**) followed by the dialkylation with n-octyl bromide using tetra butyl ammonium bromide (TBABr) as phase transfer catalyst to obtain 2,7-dibromo-9,9-dioctyl-9*H*-fluorene according to modified literature procedures[6a,8]. The dialkylateddibromo derivative of fluorene (**2**) undergoes borylation with bis(pinacolato)diboron to yield the 2,7-diboronate of fluorene intermediate (**3**) in the presence of $PdCl_2(dppf)$[9]. In a convergent way, 4-(2-ethylhexyl)-4*H*-dithieno[3,2-b:2',3'-d]pyrrole (**5**) was synthesized through dimerization of 3-bromo thiophene followed by the Buchwald-Hartwigamination approach. The synthesized intermediate (**5**) is further subjected to Vilsmeier formylation and its subsequent bromination yielded the intermediates **6** and **7** respectively. Conventional Suzuki coupling strategy was chosen to synthesize the prefinal dialdehyde derivative (**FDA**) through the connection of the intermediates **3** and **7** in the presence of $Pd(PPh_3)_4$[10]. Knoevenagel condensation of FDA with various terminal acceptor units such as N-butyl-rhodanine (**NBR**), dicyanovinylene (**DCV**) and 1,3-indanedione (**IND**) yield the target compounds namely **FD-NBR**, **FD-DCV** and **FD-IND** respectively in excellent quantity. Structures of all the compounds were confirmed using ^{1}H NMR, ^{13}C NMR, and matrix-assisted laser desorption ionization time of-flight (MALDI-TOF) mass spectrometry. The details of the experimental characterization data are available in ESI.

Photo-physical properties

The UV-visible absorption of the synthesized compounds is recorded in CH_2Cl_2 at the concentration of 1×10^{-5} M under ambient conditions. The normalized absorption and emission spectra are shown in Figure 2 and their corresponding data are compiled in Table I. We have chosen prefinal dialdehyde derivative (FDA), a reference compound in this study, to examine the optical-electro chemical characteristics of the -D-π-D- conjugated skeleton influenced by the terminal acceptor units. All compounds possess relatively broad absorption in the visible region covering the range of 300-650 nm with two primary absorption bands. The absorption bands located at shorter wavelength region is ascribed to a localized aromatic π-π* transition of the A-D-π-D-A system, while the bands at longer wavelength is

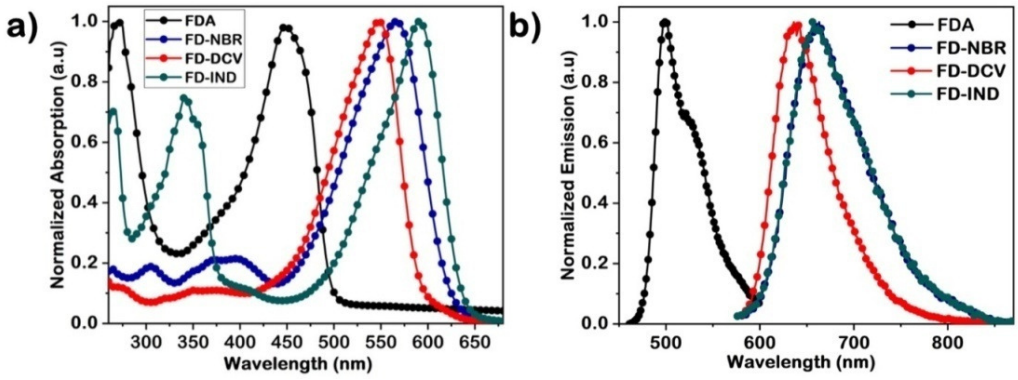

Figure 2 — (a) Normalized UV-vis absorption and (b) emission spectra of the compounds measured in CH_2Cl_2 (1×10^{-5}M) under ambient conditions

Table I — Photo-physical and electrochemical data of the synthesized donor materials

Materials	λ_{abs} (nm)[a]	ε ($M^{-1}cm^{-1}$)	λ_{film} (nm)[b]	λ_{fluo}(nm)[a]	E_{o-o} (eV)[c]	E_{ox} (V)	E_{HOMO} (eV)[d]	E_{LUMO}(eV)[e]
FD-NBR	566.4	63,233	581	657	1.99	0.86	−5.26	−3.27
FD-DCV	548.3	79,131	565	636	2.10	0.92	−5.32	−3.22
FD-IND	591.2	54,286	618	658	1.95	0.92	−5.32	−3.37
FDA	449.5	68,432		500	2.53	1.08	−5.48	−2.95

[a] Absorption and emission spectra recorded in CH_2Cl_2 solution (10^{-5} M)

[b] Absorption measured in thin film state

[c] Estimated from intersection of absorption and emission spectra in chloroform solution

[d] Reduced from the formulas $E_{HOMO} = -e[4.4 + E_{ox}]$

[e] $E_{LUMO} = [E_{o-o} - E_{HOMO}]$

mainly attributed to an ICT transition from fluorene to the terminal acceptor units. In mostly reported A-D-π-D-A systems, dicyanovinylene (DCV) end-capped compounds red shifted the absorption than N-Butyl-Rhodanine (NBR) counterparts[29,32,36, 37]. Whereas, it is found reverse in the case of A-D-π-D-A system *i.e.*, absorption of **FD-NBR > FD-DCV**, where the major ICT transition mainly originates from the DTP donor units but a limited response noticed from the central fluorene part. This observation clearly entails that shift in absorption wavelength is not only influenced by the terminal acceptors but molecular framework also plays a significant role. The absorption maxima of **FD-NBR**, **FD-DCV** and **FD-IND** are found at 566, 548 and 591 nm respectively with the molar extinction coefficients range of 54, 286-79, 131 $M^{-1}cm^{-1}$ (Figure S1, ESI). The substitution of formyl group with terminal acceptor units lead to a bathochromic shift of 98-141 nm to longer absorption wavelength. The emission maxima of **FD-NBR**, **FD-DCV** and **FD-IND** are found at 657, 636 and 658 nm respectively. The absorption spectra measured in thin film state displays a significant broadening and red shift as compared to the solution phase. This can be ascribed to the well-aligned intermolecular interactions upon film formation (Figure 3c). The optical band gap (E_{o-o}) of the compounds is estimated from the intersection of absorption and emission spectra (Fig. S2), and the values obtained are 1.99, 2.10, and 1.95 eV for **FD-NBR**, **FD-DCV** and **FD-IND** respectively (Table I).

To investigate the solvatochromic behavior of the compounds, we have measured the absorption and emission spectra in various solvents ranging from non-polar to polar aprotic and protic solvents (Figure. S3 and Table S1 and S2, ESI). Absorption profiles are impassive irrespective of solvent polarity. In emission profiles, compounds are found to exhibit bathochromic shift, recognizing the signature of positive solvatochromism. Upon increasing the polarity of solvent, strong ICT transition occurs between donor and acceptor units. Molecules undergo well stabilization and structural relaxation in the excited state by polar solvents[6b]. Non-polar locally excited (LE) state, as depicted in absorption, converted into a polar excited state[6b] in the presence of a polar aprotic/protic environment, substantiated from emission profiles. Remarkable enhancement in the dipole moment variation from ground to transient state also corroborates the positive solvatochromism for the compounds.

Electrochemical Studies

Cyclic voltammetric (CV) technique was employed to examine the energy levels and redox characteristics of the compounds using a standard three electrode configuration in the presence of tetra butyl ammonium perchlorate (0.1M) as supporting electrolyte at the scan rate of 50 mVs^{-1}. The cyclic voltammograms are displayed in Figure 3 and the corresponding data are summarized in Table I. The prefinal dialdehyde derivative (FDA) exhibited an irreversible oxidation potential at 1.08 V against standard calomel electrode and this value was taken as reference to identify the influence of terminal acceptor units on the oxidation potentials of A-D-π-D-A systems. All the compounds show oxidation potential in the range of 0.86 - 0.92 V. With respect to

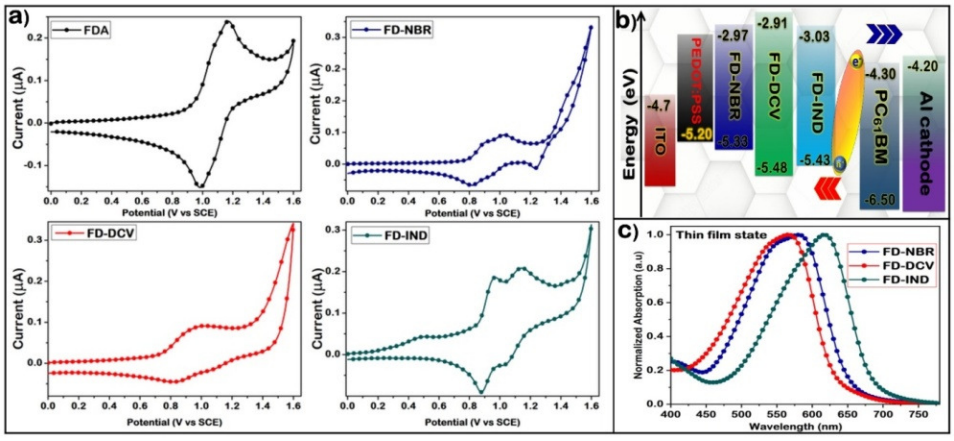

Figure 3 — (a) Cyclic voltammograms of the compounds measured in CH_2Cl_2 using standard three electrode configuration at the scan range of 50 mVs^{-1}; (b) Schematic diagram representing the energy levels of the compounds and the $PC_{61}BM$ electron acceptor; (c) Absorption profiles recorded in thin film state.

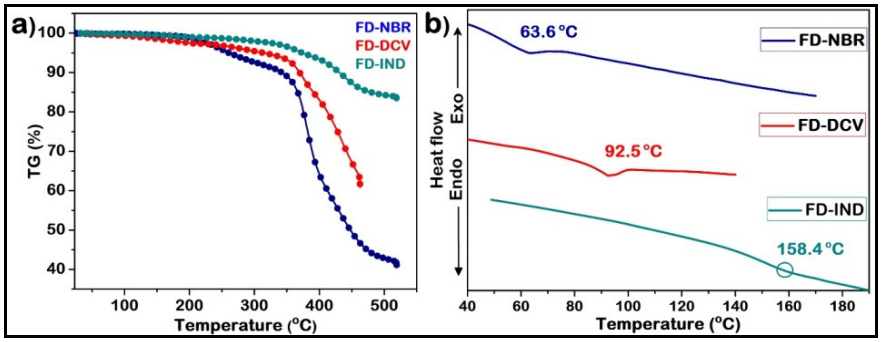

Figure 4 — TGA and DSC plots of the titled compounds showing the decomposition (T_d) and glass transition temperature (T_g) respectively recorded at a heating rate of 10 min^{-1}

the aldehyde derivative (FDA), three acceptor units do a distinctive negative shift. For instance, introduction of n-butyl-Rhodanine (NBR) and 1,3-indanedione (IND) into A-D-π-D-A system negatively shifts the oxidation potential to 0.86 V and 0.92 V respectively and both are quasi-reversible. On the other hand, **FD-DCV** shows the oxidation peak at 0.92 V which is identical to **FD-IND** but the oxidation process found to be irreversible between the anodic and cathodic potentials (Figure 3a). HOMO of all the compounds are calculated from the empirical formula: $E_{HOMO} = -e[4.4+ E_{ox}]$ eV based on SCE energy level relative to vacuum[12]. The first oxidation peak potential was used to calculate the HOMO and the obtained values are −5.26, −5.32 and −5.32 eV for **FD-NBR**, **FD-DCV** and **FD-IND** respectively. LUMO is estimated from the measured HOMO values and optical band gap. The values are calculated to be -3.27, -3.22 and -3.37 eV for **FD-NBR**, **FD-DCV** and **FD-IND** respectively. HOMO and LUMO of these SMEDs are well matched with the commonly used $PC_{61}BM$ and $PC_{71}BM$ electron acceptors (Figure 3b).

Thermal properties

The thermal properties and phase transition nature of the represented compounds have been examined using thermogravimetric analysis (TGA) and differential scanning calorimetry (DSC) respectively under nitrogen atmosphere at a heating rate of 10°C min^{-1}. All the compounds exhibited excellent thermal stability with insignificant weight loss upon 5% decomposition and values were in the range of 260-373. As depicted in Figure 4 and Table II, Glass transition temperature was determined from the second heating scan and gradually increased in the mentioned order: **FD-NBR< FD-DCV< FD-IND**. This may be originated from the well-ordered π–π interaction of terminal acceptor units with neighbouring molecules. Melting temperature (T_m) of these derivatives displayed 240, 255 and 200°C, respectively for **FD-NBR**, **FD-DCV** and **FD-IND**. The excellent thermal properties of these compounds demonstrated its potential for various optoelectronic device applications.

Table II — Thermal data of the synthesized donor materials

Materials	Glass transition temperature (T_g °C)	Decomposition temperature (T_d °C)	Melting temperature (T_m °C)
FD-NBR	63.6	260.4	240
FD-DCV	92.5	313.6	255
FD-IND	158.4	373.4	200

Conclusion

In this work, we have reported a series of three A-D-π-D-A type molecules comprised of a fluorene, dithieno[3,2- b:2',3'-d]pyrrole as common spacer and donor units respectively but with three various terminal acceptor units such as N-butyl rhodanine (for **FD-NBR**), dicyanovinylene (for **FD-DCV**) and 1,3-indanedione (for **FD-IND**)to evaluate the effect of acceptor on optical, electro chemical and thermal properties. All these compounds possess relatively broad absorption in the visible region covering the range of 300-650 nmwith high molar extinction coefficients.All the compounds exhibited excellent thermal stability with thermal decomposition temperature (T_d) as 260, 314 and 373°C, respectively for **FD-NBR**, **FD-DCV** and **FD-IND**, indicating that they are suitable for vacuum deposition fabrication technique.Their HOMO/LUMO energy levels (-5.26/-3.27 eV for **FD-NBR**, -5.32/-3.22 eV for **FD-DCV** and -5.32/-3.37 eV for **FD-IND**) of these SMEDs are well matched with the commonly used $PC_{61}BM$ and $PC_{71}BM$ electron acceptor. **FD-NBR**, **FD-DCV** and

FD-IND are showing promising properties for application in SM-BHJSCs.

Supplementary Information

Supplementary information is available in the website http://nopr.niscair.res.in/handle/123456789/60.

Acknowledgements

EAN thanks to CSIR, BMR thanks to UGC, India for financial support. VJR thanks CSIR for the Emeritus Scientist Honor. We thank Dr. K. Bhanuprakash, C&FC Division, CSIR-IICT for valuable suggestions. IICT/Pubs./2019/268.

References

1 Chen J & Cao Y, *Acc Chem Res*, 42 (2009) 1709.
2 Lin Y & Zhan X, *Acc Chem Res*, 2 (2015) 175.
3 Cheng Y J, Yang S H & Hsu C S, *Chem Rev*, 11 (2009) 5868.
4 Li G, Zhu R & Yang Y, *Nat Photonics*, 3 (2012) 153.
5 Li Y, *Acc Chem Res*, 45 (2012) 723.
6 (a) Paramasivam M, Gupta A, Raynor A M, Bhosale S V, Bhanuprakash K & Jayathirtha Rao V, *RSC Advances*, 67 (2014) 35318; (b) Gopal V R, Reddy A M & Jayathirtha Rao V, *J Org Chem*, 60 (1995) 1966.
7 Chen Y H, Lin LY, Lu C W, Lin F, Huang Z Y, Lin H W, Wang P H, Liu Y H, Wong K T, Wen J & Miller D J, *J Am Chem Soc*, 33 (2012) 13616.
8 Paramasivam M, Chitumalla R K, Singh S P, Islam A, Han L, Jayathirtha Rao V & Bhanuprakash K, *J Phys Chem C*, 30 (2015) 17053.
9 Busireddy M R, Chereddy N R, Shanigaram B, Kotamarthi B, Biswas S, Sharma G D & Vaidya J R, *Phys Chem Chem Phys*, 31 (2017) 20513.
10 Busireddy M R, Madhu C, Chereddy N R, Appalanaidu E, Sharma G D & Vaidya J R, *Chem Photo Chem*, 2 (2018) 81.
11 Lu Z, Li C, Fang T, Li G & Bo Z, *J Mater Chem A*, 26 (2013) 7657.
12 Paramasivam M, Gupta A, Babu N J, Bhanuprakash K, Bhosale S V & Jayathirtha Rao V, *RSC Advances*, 71 (2016) 66978.
13 Busireddy M R, Mantena V N R, Chereddy N R, Shanigaram B, Kotamarthi B, Biswas S, Sharma, G D & Vaidya J R, *Organic Electronics*, 37 (2016) 312.
14 Busireddy M R, Mantena V N R, Chereddy N R, Shanigaram B, Kotamarthi B, Biswas S, Sharma G D & Vaidya J R, *Phys Chem Chem Phys*, 47 (2016) 32096.
15 Busireddy M R, Chakali M, Reddy G R, Chereddy N R, Shanigaram B, Kotamarthi B, Sharma G D & Vaidya J R, *Solar Energy*, 186 (2019) 84.
16 Liu Y, Chen C C, Hong Z, Gao J, Yang Y M, Zhou H, Dou L G & Yang Y, *Scientific Reports*, 3 (2013) 3356.
17 Ni W, Wan X, Li M, Wang Y & Chen Y, *Chem Commun*, 24 (2015) 4936.
18 Wang Y L, Li Q S & Li Z S, *Computational Materials Science*, 156 (2019) 252.
19 Yuan J, Zhang Y, Zhou L, Zhang G, Yip H L, Lau T K, Lu X, Zhu C, Peng H, Johnson P A & Leclerc M, *Joule*, 4 (2019) 1140.
20 Ans M, Ayub K, Muhammad S & Iqbal J, *Computational and Theoretical Chemistry*, (2019)
21 Wen X, Xiao B, Tang A, Hu J, Yang C & Zhou E, *Chin J Chem*, 5 (2018) 392.
22 Wang Z, Zhu L, Shuai Z & Wei Z, *Macromol Rapid Commun*, 22 (2017) 1700470.
23 Liu F, Zhou Z, Zhang C, Vergote T, Fan H, Liu F & Zhu X, *J Am Chem Soc*, 48 (2016) 15523.
24 Ilmi R, Haque A & Khan M S, *Organic Electronic*, 58 (2018) 53.
25 Wan J, Xu X, Zhang G, Li Y, Feng K & Peng Q, *Energy Environ Sci*, 8 (2017) 1739.
26 Fan B, Zhang D, Li M, Zhong W, Zeng Z, Ying L, Huang F & Cao Y, *Sci China Chem*, 6 (2019) 746.
27 Meng L, Zhang Y, Wan X, Li C, Zhang X, Wang Y, Ke X, Xiao Z, Ding L, Xia R & Yip H L, *Science*, 6407 (2018) 1094.
28 Sun K, Xiao Z, Lu S, Zajaczkowski W, Pisula W, Hanssen E, White J M, Williamson R M, Subbiah J, Ouyang J & Holmes A B, *Nature Communications*, 6 (2015) 6013.
29 Sim J, Lee H, Song K, Biswas S, Sharma A, Sharma G D & Ko J, *J Mater Chem C*, 16 (2016) 3508.
30 Revoju S, Biswas S, Eliasson B & Sharma G D, *Dyes and Pigments*, 149 (2018) 830.
31 Zhao J, Xia B, Lu K, Deng D, Yuan L, Zhang J, Zhu L, Zhu X, Li H & Wei Z, *RSC Advances*, 65 (2016) 60595.
32 Antwi B Y, Taylor R G D, Cameron J, Owoare R B, Kingsford-Adaboh R & Skabara P J, *RSC Advances*, 101 (2016) 98797.
33 Deng D, Yang Y, Zou W, Zhang Y, Wang Z, Wang Z, Zhang J, Lu K, Ma W & Wei Z, *J Mater Chem A*, 44 (2018) 22077.
34 Mercier L G, Mishra A, Ishigaki Y, Henne F, Schulz G & Bäuerle P, *Org Lett*, 10 (2014) 2642.
35 Zhang Q, Kan B, Liu F, Long G, Wan X, Chen X, Zuo Y, Ni W, Zhang H, Li M & Hu Z, *Nature Photonics*, 1 (2015) 35.
36 Long G, Wan X, Kan B, Liu Y, He G, Li Z, Zhang Y, Zhang Y, Zhang Q, Zhang M & Chen Y, *Adv Energy Mater*, 5 (2013) 639.
37 Lee H, Jo H, Kim D, Biswas S, Sharma G D & Ko J, *Dyes and Pigments*, 129 (2016) 209.
38 Wang W, Shen P, Dong X, Weng C, Wang G, Bin H, Zhang J, Zhang Z G & Li Y, *ACS Appl Mater Interfaces*, 5 (2017) 4614.
39 Carsten B, Szarko J M, Son H J, Wang W, Lu L, He F, Rolczynski B S, Lou S J, Chen L X & Yu L, *J Am Chem Soc*, 50 (2011) 20468.